Precision Engineering 65 (2020) 103–115

Contents lists available at ScienceDirect

Precision Engineering

journal homepage: http://www.elsevier.com/locate/precision

Systematic approach to realizing optimal moving order selection for multi-axis precise motion system

Hao Tang [a,*], Zilin Zhang [b]

[a] Hunan University of Science and Technology, College of Mechanical Engineering, Xiangtan, Hunan, China
[b] Lund University, Faculty of Engineering, Lund, Sweden

ARTICLE INFO

Keywords:
Optimal moving order selection
Multi-axis precise motion platform
Error analysis
Error modelling
Orthogonal test

ABSTRACT

This paper presents a systematic approach for selecting the optimal moving order (MO) in a multi-axis precise motion system (MPMS). According to the proposed procedure, an optimal high-efficiency MO selection approach for high-efficiency and high-accuracy requirement is introduced. First, the characteristics of the giving MPMS are analysed, and the error model is established. The orthogonal test method is used to evaluate the influence on the MO caused by different MPMS configurations. Second, the number of possible MOs can be narrowed to limited and satisfied MO types. By calculating the deviations after each step, all directional movements can be arranged. Third, considering that both the accuracy and efficiency are important indexes, a series of systematic formulations are developed to select the optimal MO to balance accuracy and efficiency. A case for which a six-axis precise platform is adopted in an optoelectronic packaging system is implemented, and the methods of high-quality MO selection are verified by performing a series of experiments, and the methods are shown to be useful and effective. To balance the proportion of efficiency and accuracy, the formula and corresponding model are proposed to select the MO. The approach is not only beneficial to the accuracy improvement and trajectory planning of MPMS, but also helpful in terms of reducing the computational processing for the following algorithm. For the engineers using in precise industry area, the proposed approach can significantly improve the operative precision of MPMS with an optimal MO. This methodology of MO can also be the basis of references to error-related analyses on MPMS.

1. Introduction

Multi-axis precise motion systems (MPMSs) are widely used in high-accuracy motion control systems, such as optoelectronic packaging systems (OPS), robotics control systems and aerospace engineering for specific engineering tasks. MPMS contains several degrees-of-freedom (DOFs) to control a giving object moving from one position to another position precisely. There are different errors which contribute to the orientation deviation, and there is a large number of moving orders (MO) [1]. A good moving order can not only improve the systematic accuracy but can also reduce the computational processing for the following algorithm. Furthermore, an optimal MO can guarantee the efficiency and accuracy for different environments, and MO analysis is beneficial to the trajectory planning of MPMS. Therefore, the selection of an optimal MO for MPMS in motion control is very important, especially for the precise engineering industries.

Recently, there have been limits in the error analysis and MO approach for MPMS. Most researchers have focused on the error modelling procedure for multi-axis systems, and the application of error models, as well as error prediction and compensation has attracted little attention. Hale [2] introduced the principles and techniques for multi-axis precision machines in his dissertation, and it focused on error modelling procedures, error prediction as well as compensation and related mathematical tools. However, there has been little attention on sensitivity analysis, configuration optimization and MO selection. Since the beginning of this century, an increasing number of researchers have focused on the error analysis for multi-axis machine tools. Tang [3] proposed an integrated geometric error modelling, identification, and compensation for multi-axis system. Vogl [4] used an inertial measurement unit for on-line machine condition monitoring, which can be applied to smart machines and provide actionable intelligence to manufacturers. Yang [5] applied screw theory to the machining precision analysis and prediction of multi-axis CNC machine tools. Zhong [6] proposed an error transfer relationship model which can be used to optimize manufacture translational axes. In addition, the research on the

* Corresponding author.
E-mail address: tanghao@hnust.edu.cn (H. Tang).

https://doi.org/10.1016/j.precisioneng.2020.05.007
Received 5 October 2019; Received in revised form 18 May 2020; Accepted 20 May 2020
Available online 24 May 2020
0141-6359/© 2020 Elsevier Inc. All rights reserved.

Nomenclature

MPMS	Multi-axis precise motion system
OPS	Optoelectronic Packaging System
DOF	Degree of freedom
HTM	Homogeneous Transformation Matrix
X, Y, Z, A, B, C	Axis in MAS
x, y, z, A, B, C	Geometric error
$x^k, y^k, z^k, A^k, B^k, C^k$	Kinematic error
$\alpha^a, \beta^a, \gamma^a$	Assembly error
M^c	Coordinate offset matrix
M^{mov}	Movement matrix
E^k	Kinematic error matrix
E^a	Assembly error matrix
OPL	Optical power loss
MO	Moving order
ω	Weighting accuracy parameter
μ	Weighting efficiency parameter
PL_w, PL_j	The highest and lowest accuracy values
A_w, A_j	The highest and lowest efficiency values

trajectory analysis of optoelectronic packaging systems has attracted interest recently, and has led to new areas of focus to increase the machining quality of MPMS. Huang [7] proposed a real-time federate scheduling approach for five-axis machine tools, which is beneficial for linear and angular trajectory planning. Tseng [8] modified a conventional method to plan the trajectory for the automatic alignment of fibre-optic. The Hamiltonian [9] algorithm and pattern search algorithm can be utilised for multiple-dimensional blind searching of trajectories in aligning systems, while the hill climbing method is limited for one-dimensional (1D) blind searching. An automated optical system [10] was designed to plan trajectories avoiding blind calibration during optical fibre alignment, and to increase the time efficiency for alignment. Wang [11] developed a corner trajectory smoothing approach with an asymmetrical transition profile for CNC machine tools. He also discussed the effect of the velocity, acceleration, and jerk limits for each axis. However, even though the machining accuracy was considered, the MO was not considered. Some common applications are error prediction, compensation, and error sensitivity analysis, while the MO analysis and configuration optimization are also important. Van [12] proposed a dynamic model of multi-axis machines with multiple different configurations. He also used a coordinate transformation method to simulate various configurations of machine tools. However, this method is limited only to machine tools with certain configurations. Wang [13] designed the configuration for a grinding machine tool. He reported that an unsuitable configuration can impede the trajectory planning of grinding. Although this paper shows that the configuration of a machine tool can affect the precision of the machine's operation, this area has not been extensively developed.

There is usually a feedback module in motion control systems, and an optimal trajectory and lower deviation orientation are also helpful for successive procedures. An optimal MO can not only reduce the deviation, but it can also improve the efficiency in the motion process. In conclusion, although most researchers focused on error prediction and compensation based on error analysis, the MO for multi-degree of freedom (DOF) motion systems requires more attention.

In this paper, a novel approach for developing the optimal MO for MPMS is introduced. Section 2 presents the methodology of the proposed approach. Then, Section 3 proposes a case in a laser welding system, including the simulation procedure and experimental results, which proves the optimal MO selection approach.

2. Methodology

Generally, a typically MPMS consists of 6 DOFs. The three translational axes are referred to as the X, Y, and Z axes, and the three rotational axes are called the A, B, and C axes. There are several groups of errors, including the geometric error, thermal error, and load effects. Compared to the machine tools, the MPMS has some characteristics, including small scale, high accuracy and good environmental conditions. It is widely utilised in the laboratory, so the temperature and humidity can be kept in balance. Although the thermal effect in numerical machining centre is great, because there is no fabrication in the MPMS moving process, the geometric error plays a dominant role in the orientation of a target object fixed on the MPMS. The geometric error is categorized into two groups, namely the kinematic error and assembly error. The kinematic error is generated during motion, and the assembly error is generated during installation. Further, two types of parameters are considered, namely the coordinate offset and the movement.

Ideally, a different MO results in the same orientation without considering the errors. However, depending on the effect of all geometric errors, a different MO of a giving MPMS will result in a different orientation deviation of the object controlled by MPMS [14]. Therefore, it is necessary to develop an optimal MO, which benefits the procedure in terms of accuracy and efficiency.

In this paper, a novel MO selection approach is proposed for MPMS in precise orientation control. The procedure for selecting the optimal MO is introduced below.

1. Error modelling for MPMS. To calculate the deviations, it is necessary to transform the error issue into a mathematical problem. The homogeneous transformation matrix (HTM) is utilised and is considered a mathematical tool to denote the orientation. All matrices are listed in Table 1.

where *c*, *mov*, *a* and *k* denote the coordinate offset matrix, movement matrix, assembly error matrix and kinematic error matrix, respectively. The ideal condition only considers the coordinate offset matrix and the movement matrix, and the actual condition should consider the extra part, the kinematic error matrix, and the assembly error matrix.

Considering that the matrix multiplication order does not follow the Commutative Law, the ideal and the actual orientation of the object are derived as in Eq. (1) and Eq. (2).

$$\boldsymbol{E}_{0n}^{i} = \boldsymbol{P}_0 \prod_{j=0}^{n} \boldsymbol{M}_{jj+1}^{c} \boldsymbol{M}_{jj+1}^{mov} \tag{1}$$

$$\boldsymbol{E}_{0n}^{a} = \boldsymbol{P}_0 \prod_{j=0}^{n} \boldsymbol{M}_{jj+1}^{a} \boldsymbol{E}_{jj+1}^{a} \boldsymbol{M}_{jj+1}^{mov} \boldsymbol{E}_{jj+1}^{k} \tag{2}$$

where *i* and *a* denote the ideal state and actual state, respectively.

Based on the subtraction of the two equations, the real orientation deviation can be calculated as shown in Eq. (3).

$$\boldsymbol{E} = \boldsymbol{E}_{0n}^{a} - \boldsymbol{E}_{0n}^{i} \tag{3}$$

Eq. (3) denotes the error model of a giving MPMS. The orientation deviations with different movement can be calculated using the error model. The error modelling part can be regarded as the mathematical base for obtaining the orientation deviation and developing the optimal MO. To reduce the computational volume, an orthogonal test is adopted to select different possible configurations.

2. Configuration analysis. It is important to first analyse the configuration of MPMS, including the number of DOFs, the number of sensitive and insensitive DOFs, the comprehensiveness, and informativeness of the optimal MO selection method.

Table 1
Matrices and corresponding physical meanings.

Coordinate offset matrix	Movement matrix for A unit	Assembly error matrix	Kinematic error matrix
$\boldsymbol{M}^c = \begin{bmatrix} 1 & 0 & 0 & x_c \\ 0 & 1 & 0 & y_c \\ 0 & 0 & 1 & z_c \\ 0 & 0 & 0 & 1 \end{bmatrix}$	$\boldsymbol{M}_A^{mov} = \begin{bmatrix} 1 & 0 & 0 & 0 \\ 0 & \cos\alpha_A & -\sin\alpha_A & 0 \\ 0 & \sin\alpha_A & \cos\alpha_A & 0 \\ 0 & 0 & 0 & 1 \end{bmatrix}$	$\boldsymbol{E}_A^a = \begin{bmatrix} 1 & -\Delta\gamma_A^a & \Delta\beta_A^a & 0 \\ \Delta\gamma_A^a & 1 & -\Delta\alpha_A^a & 0 \\ -\Delta\beta_A^a & \Delta\alpha_A^a & 1 & 0 \\ 0 & 0 & 0 & 1 \end{bmatrix}$	$\boldsymbol{E}_A^k = \begin{bmatrix} 1 & -\Delta\gamma_A^k & \Delta\beta_A^k & \Delta x_A^k \\ \Delta\gamma_A^k & 1 & -\Delta\alpha_A^k & \Delta y_A^k \\ -\Delta\beta_A^k & \Delta\alpha_A^k & 1 & \Delta z_A^k \\ 0 & 0 & 0 & 1 \end{bmatrix}$

For a multi-axis system, there are $n!$ (n means the number of degree-of-freedom) configurations available. However, there are only one, or one group of configuration can meet the requirement, accuracy or efficiency. Thus, it is necessary to consider the effect of configuration, and develop an optical one. In this paper, the orthogonal test is utilised in configuration analysis. First, it is necessary to develop the sensitive deviation. In most cases, not all directional deviations are in the same level. Second, all configurations are named and several possible configurations are raised. Third, the several configurations are compared in the following MO analysis. A specific case of configuration analysis is introduced in 'Case Study'.

3. Error sensitivity analysis. The sensitivity is defined as the gradient (increasing rate) of deviation. For most cases, not all DOFs have the same sensitivity levels, and it depends on the specific requirements. Thus, it is necessary to develop the sensitivity order for all sensitive DOFs. Considering that all errors follow the Gaussian distribution, the influence of each DOF is monotonous in the single side (there is only one extreme value for all errors in the distribution).
4. Accuracy arrangement. To develop the most accurate MO, each sensitive DOF is evaluated individually. Assume that the first step is the evaluated DOF, and the other sensitive DOFs are arranged separately in step 2. Therefore, the deviations by the evaluated DOF movement in the first step can be obtained. On the other hand, the two steps are reversed. Assume that the second step is the evaluated DOF, and the first step is the other sensitive DOF. Similarly, the deviations by the evaluated DOF movement in the second step can be obtained as well. If the deviations of the evaluated DOF in the first step are larger than those in the second step, the evaluated DOF is set at the start of the MO. On the contrary, the evaluated DOF is set at the end of the MO. Thus, one DOF is arranged for the moving order, and the other DOFs can be developed individually. Considering that there are several DOFs at the beginning or the end of the MO, the sensitivity order in step 2 can be adopted to list the order.

For example, there is an MPMS with K DOFs which contains n sensitive DOFs and m insensitive DOFs. The sensitivity analysis result is shown in Eq. (4).

$$I_1 > I_2 > \cdots > I_i = I_j > \cdots > I_n \tag{4}$$

where I denotes the sensitivity index, I_1 and I_n denote the highest and lowest sensitivity DOF, respectively, and I_i and I_j denote the DOFs with the same sensitivity level.

If i is the evaluated DOF, it is first set in step 1, and other DOFs are set in step 2 separately.

$$(I_i, I_1), (I_i, I_2), \cdots (I_i, I_{i-1}), (I_i, I_{i+1}), \cdots (I_i, I_n) \tag{5}$$

Therefore, there are n-1 groups, and the average deviations after the evaluated DOF (step 1) can be obtained and is referred to as D_1.

Similarly, i is set in the second step, and the other DOFs are set in step 1 separately,

$$(I_1, I_i), (I_2, I_i), \cdots (I_{i-1}, I_i), (I_{i+1}, I_i), \cdots (I_n, I_i) \tag{6}$$

The average deviations after the evaluated DOF (step 2) can also be obtained, and are called D_2. If D_1 is larger than D_2, the DOF i is set at the beginning of the MO. On the contrary, if D_1 is smaller than D_2, the DOF i is set at the end of the MO. The specific order for multi DOFs at the beginning or end is according to the sensitivity order, i.e. I_1 is ahead of I_2 at the beginning, or behind I_2 at the end.

After arranging the DOF I, other DOFs can be arranged using the same procedure. If there are several DOFs at the beginning or end, the variation in the speed of the DOF can be adopted accordingly. The variation in the speed of the DOF i is shown in Eq. (7).

$$S_i = D_1^i - D_2^i \tag{7}$$

where S denotes the increasing rate. If the changing speed order of DOF is:

$$S_1 > S_2 > \cdots > S_i = S_j > \cdots > S_n \tag{8}$$

The fastest-changing DOF should be first arranged, i.e. S_1 is ahead of S_2 at the beginning, and S_n is behind by S_2 at the end.

5. Efficiency arrangement. In some cases, the efficiency is also important when arranging MOs. To develop the most efficient MO, the sensitive order can be obtained in the first step. If the deviation caused by the X unit is close to the deviation of the Y unit, then the X and Y units are defined as similar units. Assuming that the order of sensitivity is X>Y>A>B, then the optimal MO is arranged as B-A-Y-X. If there are similar units DOF i and DOF j in a given order, the increasing rates of similar units should be considered. The other units should be first arranged, and the selection scale is defined, after which similar units are arranged. The average deviations of the DOF i in two steps within the selection scale are denoted by D_1^i and D_2^i. The varying speed of i is S_i (see Eq. (7)). The average deviations of DOF j in two steps within the selection scale are denoted by D_1^j and D_2^j. The variation in the speed of j can be obtained as S_j. If S_i is larger than S_j, DOF i should be set at the back of j. If S_i is smaller than S_j, DOF i should be set at the front of j.
6. Balance of efficiency and accuracy. Generally, to select an optimal MO for a given MPMS, both the accuracy and efficiency should be considered. Fig. 1 shows how to narrow the range from a large number of possible *MO*s. For the systematic accuracy of a given MPMS, two boundaries exist, i.e. the highest and lowest boundaries. For the sake of accuracy, they are represented by PL_w and PL_j, and for efficiency, they are represented by A_w and A_j, respectively. Considering the different characteristics of MPMS, there is a floating point MO_k sliding along the line PL_wPL_j, as shown in Fig. 1(a). If the accuracy requirement is sharp, the range of MO_kPL_j will be narrow, which means that the satisfied *MO* types are small. On the contrary, if the accuracy requirement is soft, the range of MO_kPL_j will be wide, which means that the satisfied *MO* types are large. Similarly, the procedure for the efficiency can also be derived, as shown in Fig. 1 (b).

To develop the process, an accuracy weighing parameter ω and an efficiency weighing parameter μ are adopted. If there are no requirements, ω and μ are equal to 1. If the accuracy and efficiency requirement are sharp, $\omega > 1$ and $\mu > 1$, so the range of MO_kPL_j and A_kPL_j is narrow, and the satisfied MO types are small. If the accuracy and efficiency requirements are soft, $\omega < 1$ and $\mu < 1$, so the range of MO_kPL_j and A_kPL_j is wide, and the satisfied MO types are large. Finally, by combining the satisfied MO types in terms of accuracy and efficiency,

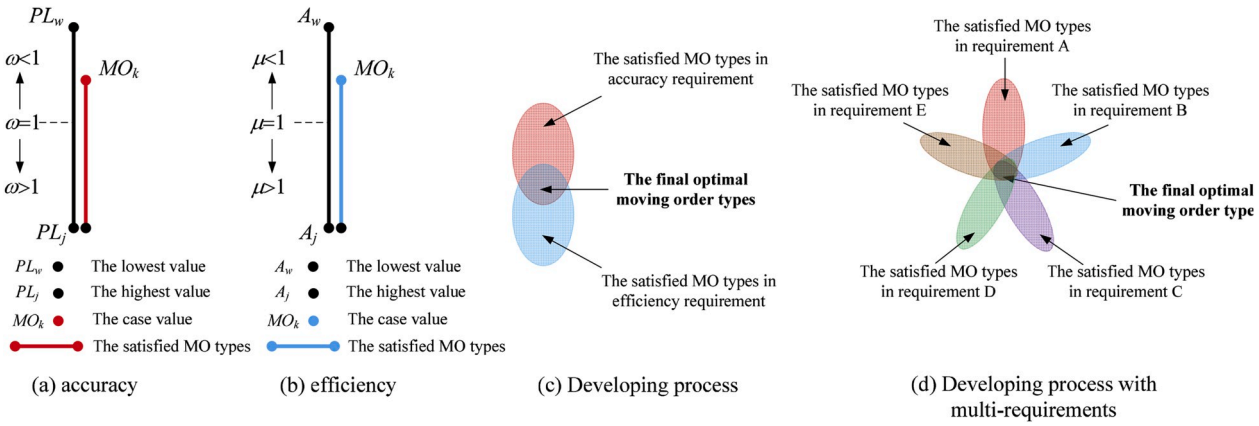

Fig. 1. Schematic for MO selection with different requirements.

the optimal MO can be developed, as shown in Fig. 1(c). Eqs. (9) and (10) explain the process mathematically.

$$\begin{cases} MO_{PL} = \left\{ MO_k \middle| \omega \dfrac{PL_k - PL_j}{PL_w - PL_j} < \dfrac{1}{2} \right\} \\ MO_A = \left\{ MO_k \middle| \mu \dfrac{A_k - A_i}{A_w - A_i} < \dfrac{1}{2} \right\} \end{cases}, k \in [0, n] \tag{9}$$

$$MO_{optimal} = \{MO_k | MO_{PL} \cap MO_A\} \tag{10}$$

For instance, if there are multiple requirements, as shown in Fig. 1 (d), the process is also applicable for developing the optimal MO types.

The procedure for developing the optimal MO is shown in Fig. 2.

3. Case Study – MPMS in laser welding system

A six-axis platform is utilised in a laser welding system (LWS), which is a high-accuracy optical device manufacturing system. The LWS contains several modules, as shown in Fig. 3.

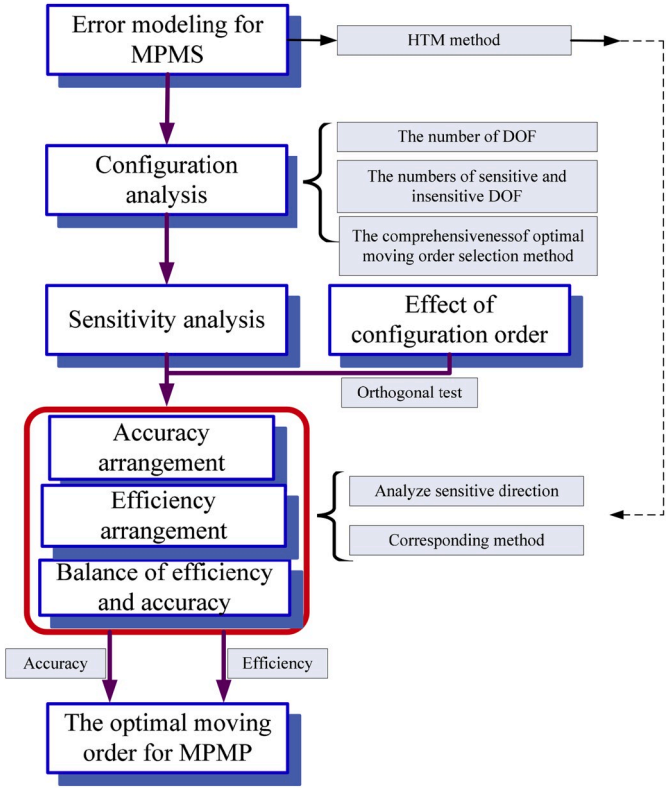

Fig. 2. Procedure for developing the optimal MO for MPMS.

The optical device manufacturing process is shown in Fig. 4. It involves the aligning and welding of two main parts. The MPMS plays a critical role in the LWS by precisely controlling the two components being aligned together.

It is clear that different MOs can result in a large difference in the orientation of the optical device manufacture process. Thus, it is necessary to accurately and effectively develop an optimal MO for the MPMS in the alignment.

3.1. Characteristics of the MPMS in LWS

In the alignment between the two components, there are two types of errors, namely the transverse dislocation and axial angle.

Generally, the optical power loss (OPL) is adopted to describe the quality of an optical device in the LWS. If the OPL is high, the quality of the optical device is poor. Fig. 5 shows the relationship between the five directional movements and the OPL. Based on Mukhopadhyay's research [15] on the coupling of a single-mode fibre to a laser diode, the formula to express the coupling efficiency is given as below.

$$\eta = \frac{\left| \int \psi_v \psi_f^* dxdy \right|^2}{\int |\psi_v|^2 dxdy \int |\psi_f|^2 dxdy} \tag{11}$$

$$PL = -10 \cdot lg\eta \tag{12}$$

Where $\Psi_v(x, y, z)$ (short as Ψ_v) denotes the deviations at X and Y axis, $\Psi_f(A, B)$ (short as Ψ_f) denotes the deviations at A and B axis, η denotes the coupling efficiency. Considered that the alignment between fiber array and the waveguide chip is centralized around Z axis, there is no efficiency loss in C axis theoretically. Z directional deviation is less sensitive than X and Y axis.

According to Yang's research [16], the X and Y directional deviations are considered transverse dislocations, and the A and B directional deviations are considered the axial angle. The two directional deviations are equal. Therefore, the sensitive indexes are X, Y and A, B directional deviations.

3.2. Error modelling procedure

Considering the environmental conditions and the characteristics of the stage, the geometric errors in MPMS play a dominate role in LWS. There are two types of geometric errors in the six-axis platform, $6 \times 6 = 36$ kinematic error terms, and $3 + 3 + 2 \times 3 = 12$ static error terms, as Table 2 and Table 3 shows.

Eq. (1) to Eq. (3) explains the error modelling procedure between two adjacent units. For a six-axis system, it is necessary to raise the

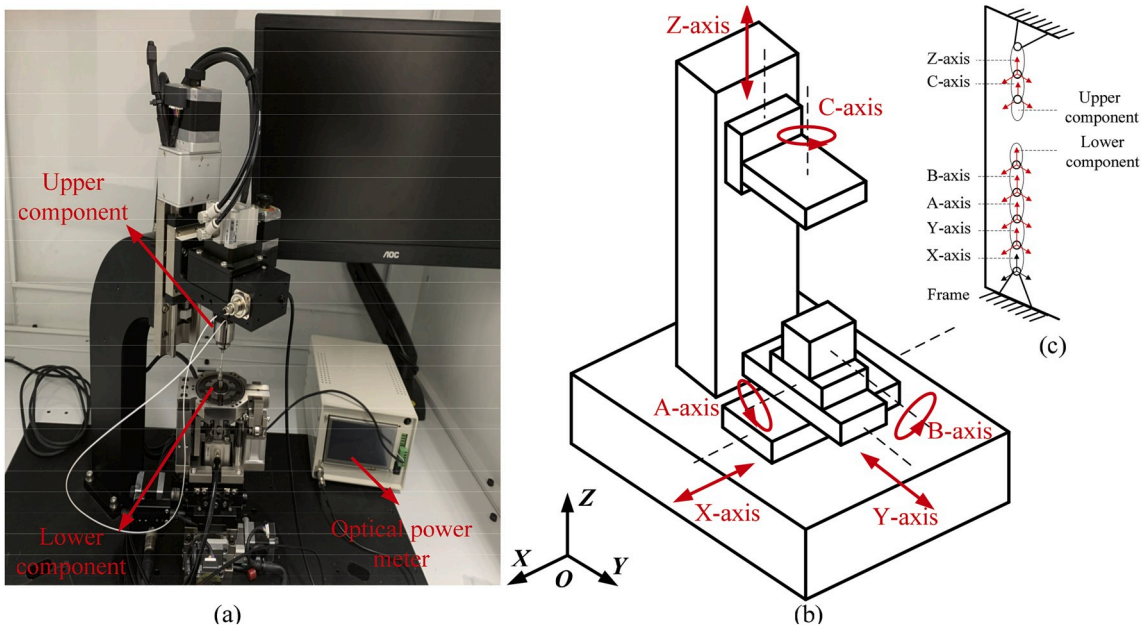

Fig. 3. Arrangement of a typical MPMS in laser welding system.

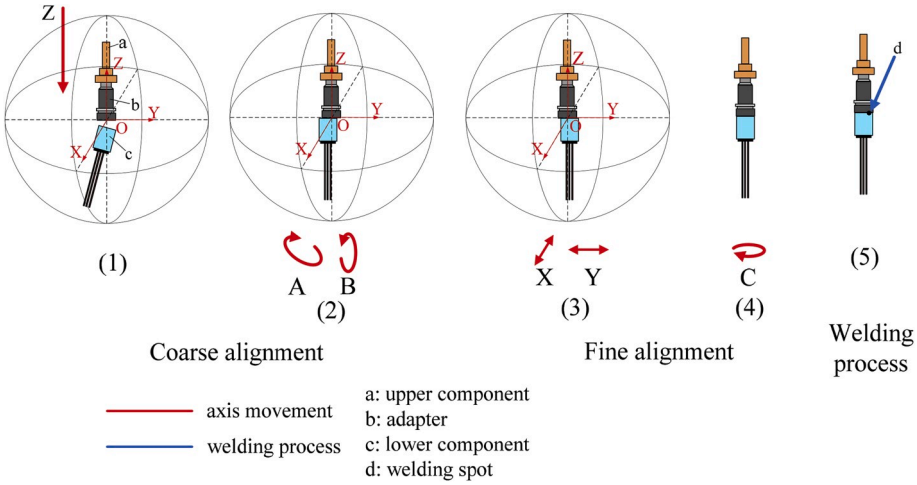

Fig. 4. Optical device manufacture procedure in LWS.

configuration first. Then the corresponding matrices can be added into the error model.

Based on the configuration C-Z-O-X-Y-A-B, the orientation of the upper component can be derived as follows:

$$\boldsymbol{E}_{0n}^{au} = \boldsymbol{P}_0 \prod_{j=0}^{n} \boldsymbol{M}_{jj+1}^{o} \boldsymbol{M}_{jj+1}^{s} \boldsymbol{M}_{jj+1}^{mov} \boldsymbol{M}_{jj+1}^{k} \ldots\ldots (n=2)$$
$$= \boldsymbol{P}_0 \boldsymbol{M}_{0z}^{c} \boldsymbol{E}_{0z}^{a} \boldsymbol{M}_{0z}^{mov} \boldsymbol{E}_{0z}^{k} \boldsymbol{M}_{zC}^{c} \boldsymbol{E}_{zC}^{a} \boldsymbol{M}_{zC}^{mov} \boldsymbol{E}_{zC}^{k} \quad (13)$$

And the orientation of the lower component can be derived:

$$\boldsymbol{E}_{0n}^{al} = \boldsymbol{P}_0 \prod_{j=0}^{n} \boldsymbol{M}_{jj+1}^{o} \boldsymbol{M}_{jj+1}^{s} \boldsymbol{M}_{jj+1}^{mov} \boldsymbol{M}_{jj+1}^{k} \ldots\ldots (n=4)$$
$$= \boldsymbol{P}_0 \boldsymbol{M}_{0x}^{c} \boldsymbol{E}_{0x}^{s} \boldsymbol{M}_{0x}^{mov} \boldsymbol{E}_{0x}^{k} \cdot \boldsymbol{M}_{xy}^{c} \boldsymbol{E}_{xy}^{s} \boldsymbol{M}_{xy}^{mov} \boldsymbol{E}_{xy}^{k} \cdot \boldsymbol{M}_{yA}^{c} \boldsymbol{E}_{yA}^{s} \boldsymbol{M}_{yA}^{mov} \boldsymbol{E}_{yA}^{k} \cdot \boldsymbol{M}_{AB}^{c} \boldsymbol{E}_{AB}^{s} \boldsymbol{M}_{AB}^{mov} \boldsymbol{E}_{AB}^{k} \quad (14)$$

By subtracting the two orientations, the orientation deviations for the two components can be obtained as follows.

$$\boldsymbol{E} = \boldsymbol{E}_{0n}^{au} - \boldsymbol{E}_{0n}^{al} \quad (15)$$

3.3. Effect of configuration order

This section discusses the characteristics of common structural configurations with six units, namely X, Y Z, A, B and C units. Using the methodology in Section 2, the orthogonal test theory is introduced to perform the configuration analysis. First, the sensitivity of the DOFs are defined in the configuration. According to Tang's research [17], deviations caused by the motions on the X, Y, A and B units are much greater than those caused by motions on the Z and C units. Thus, X, Y, A and B units can be categorized as having sensitive DOFs, and the Z and C units are arranged as having an insensitive DOF. Based on these definitions, translational units X and Y are denoted by the symbol T, rotational units U and V are denoted by R, and the Z and C units are denoted by I (insensitive factor). Considered that there are six DOFs in MPMS, 720 configurations can be named for an MPMS. To reduce the

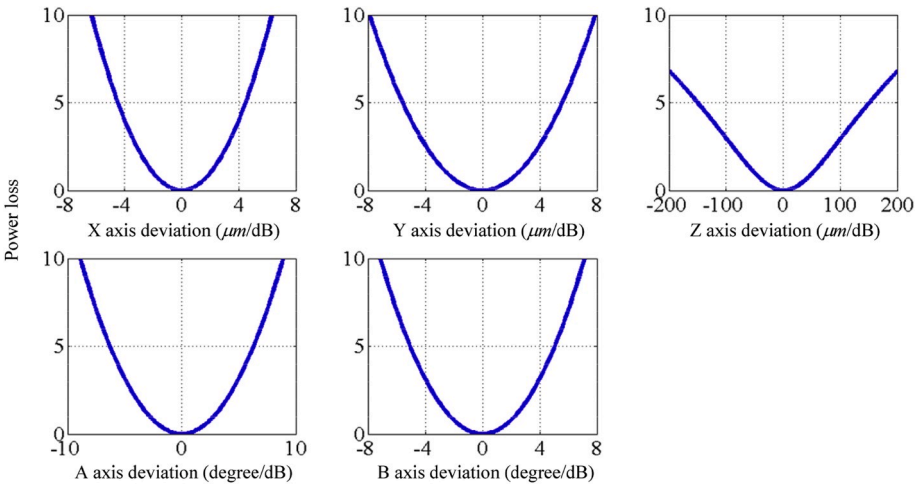

Fig. 5. Relationship between different deviations and power loss.

Table 2
Physical meaning of kinematic errors.

Axis	Error components				
	Positioning error	Straightness error	Pitch	Yaw	Roll
X-axis	x^k_x	y^k_x, z^k_x	β^k_x	γ^k_x	α^k_x
Y-axis	y^k_y	x^k_y, z^k_y	γ^k_y	α^k_y	β^k_y
Z-axis	z^k_z	x^k_z, y^k_z	α^k_z	β^k_z	γ^k_z
	Axial error	Radius error	Angular error	Tilt error	
A-axis	x^k_A	y^k_A, z^k_A	α^k_A	β^k_A, γ^k_A	
B-axis	y^k_B	x^k_B, z^k_B	β^k_B	α^k_B, γ^k_B	
C-axis	z^k_C	x^k_C, y^k_C	γ^k_C	α^k_C, β^k_C	

Table 3
Physical meaning of static errors.

Error	Axis	Error	Axis
α^s_x	X-axis	α^s_A	A-axis
β^s_y	Y-axis	β^s_B	B-axis
γ^s_z	Z-axis	γ^s_C	C-axis
α^s_{zC}, β^s_{zC}	Non-orthogonality between a translational axis and corresponding rotational axis		
α^s_{yB}, γ^s_{yB}			
β^s_{xA}, γ^s_{xA}			

computational volume in the selection, an orthogonal test is implemented. Each DOF can be regarded as a position, and there are three levels, T, R and I.

The test is arranged using the $L_{18}(3^7)$ orthogonal test table, and the results are listed in Table 4, where 0 indicates a false configuration order, and 1 indicates a correct configuration order.

The Capital letter T contains X and Y axes, R contains A and B axes, and I contains two insensitive axes Z and C axes. According to the results, only #6, #7, #10, #13 and #17 configurations can meet the requirement, marked by '1', and the degree-of-freedoms in other configurations are inappropriate. Based on the results of the orthogonal test [17], the configurations chosen are T-I-I-R-R-T, I-R-T-R-I-T, R-R-I-I-T-T, T-R-T-I-R-I and I-T-R-I-R-T, then the simulations are implemented on MPMS with the configurations X-C-Z-A-B-Y, C–B-X-A-Z-Y, A-B-Z-C-Y-X, Y-A-X-C-B-Z and Z-Y-B-C-A-X, separately. For the translational motion unit, the main error generated while moving is the positioning error, and for the rotational motion unit, the main error generated while moving is the angular error. Besides, because the positioning error of the Z motion unit and the angular error of the C motion unit are insensitive to OPL, the two motions are not considered.

Overall, this experiment is arranged such that 4! = 24 MOs of X, Y, A and B motion units are implemented on the MPMS with the five previously mentioned configurations. According to the calculation results in Eq. (13) to Eq. (15), a 1 μm displacement on the translational axis results in OPL with the same order of magnitude as a 2° angular displacement on the rotational axis. To amplify the differences between the aligning qualities of various MOs in the alignment, the step length on the translational axis is 100 μm, and the angular step length on the rotational axis is 0.5°.

Table 4
Orthogonality test results.

Experimental No.	1	2	3	4	5	6	Result
1	R	R	R	R	R	R	0
2	R	T	T	T	T	T	0
3	R	I	I	I	I	I	0
4	T	R	R	T	T	I	0
5	T	T	T	I	I	R	0
6	**T**	**I**	**I**	**R**	**R**	**T**	**1**
7	**I**	**R**	**T**	**R**	**I**	**T**	**1**
8	I	T	I	T	R	I	0
9	I	I	R	I	T	R	0
10	**R**	**R**	**I**	**I**	**T**	**T**	**1**
11	R	T	R	R	I	I	0
12	R	I	T	T	R	R	0
13	**T**	**R**	**T**	**I**	**R**	**I**	**1**
14	T	T	I	R	T	R	0
15	T	I	R	T	I	T	0
16	I	R	I	T	I	R	0
17	**I**	**T**	**R**	**I**	**R**	**T**	**1**
18	I	I	T	R	T	I	0

The OPL values of MO Y-X-B-A follow the same trend, and after step 2, the deviations between each configuration are distinct. The configuration quality for MO Y-X-B-A is arranged as Z-Y-B-C-A-X> Y-A-X-C-B-Z> X-C-Z-A-B-Y> C–B-X-A-Z-Y> X-C-Z-A-B-Y. In Fig. 6, the general trends are the same for different MOs. Then, combined with Table 5, the MOs in the same motion steps have different configurations, but the differences in the OPL values are not significant.

Similarly, all MOs have the same trends for five configurations, as shown in Fig. 6(a) to (d).

The 24 types of MO for five configurations indicate that there is little influence on each MO, and the OPL distribution of MOs and the analysis on the MO is hardly affected by the configuration order. This means that the optimal MO selection method is comprehensive and can be applied to any configuration.

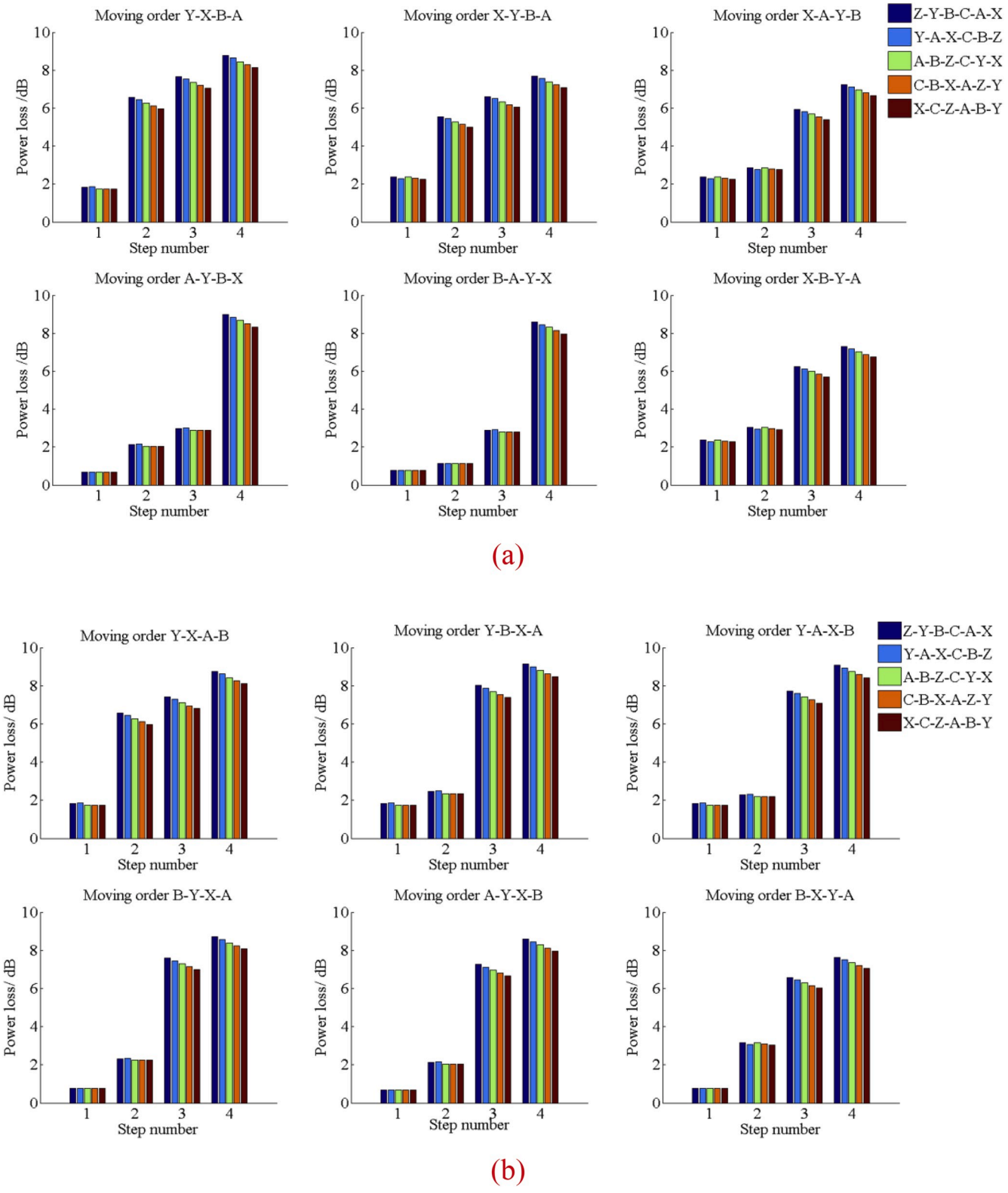

Fig. 6. OPL curves with 24 types of MO in five configurations.

3.4. Optimal MO selection

For most cases, there is a large number of MOs. Ideally, each MO can meet the requirement without considering the errors. However, because of the effects of the geometric error, a different MO can result in different orientation deviations. Therefore, it is necessary to develop an optimal MO to reduce the deviation.

Because X, Y and A, B are sensitive indexes, 24 cases of MOs having X, Y, A and B motion units are implemented. It is assumed that if there are n_1 mm in the X direction, n_2 mm in the Y direction, n_3 degrees in the

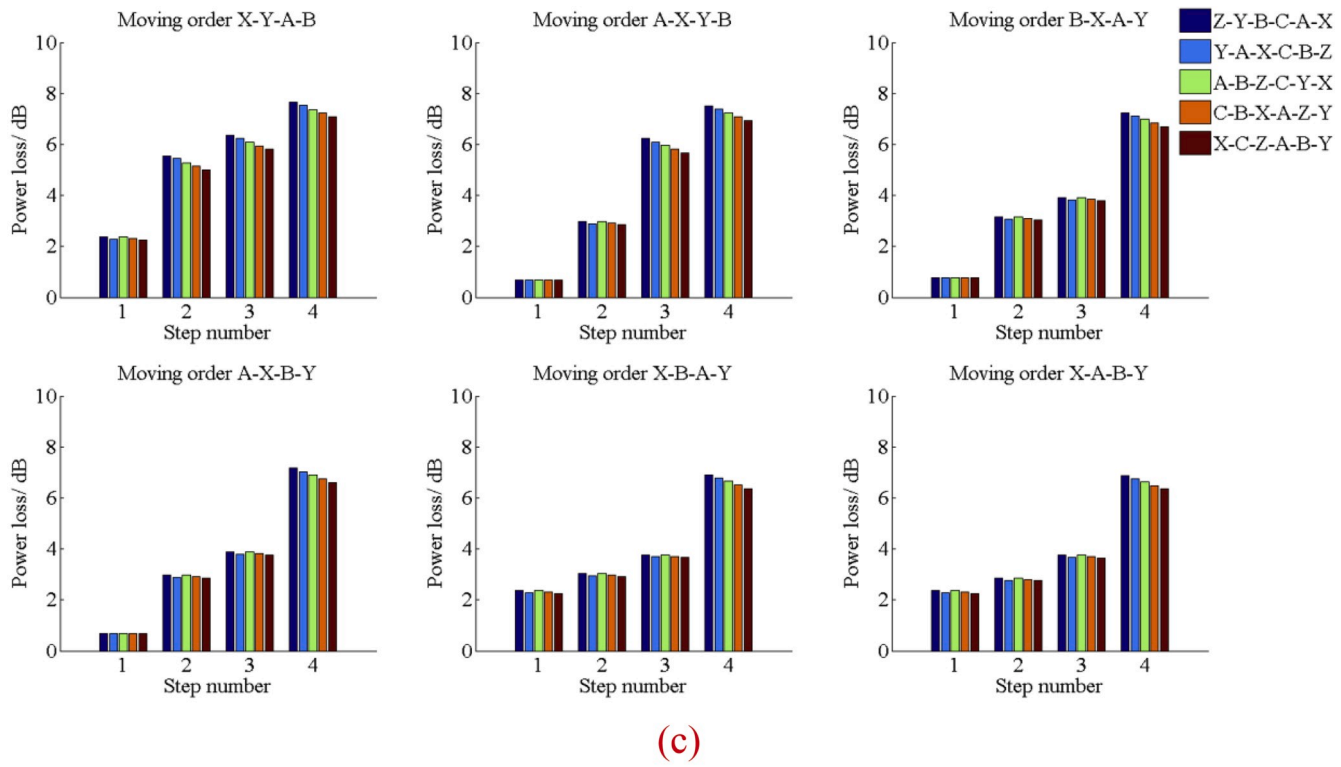

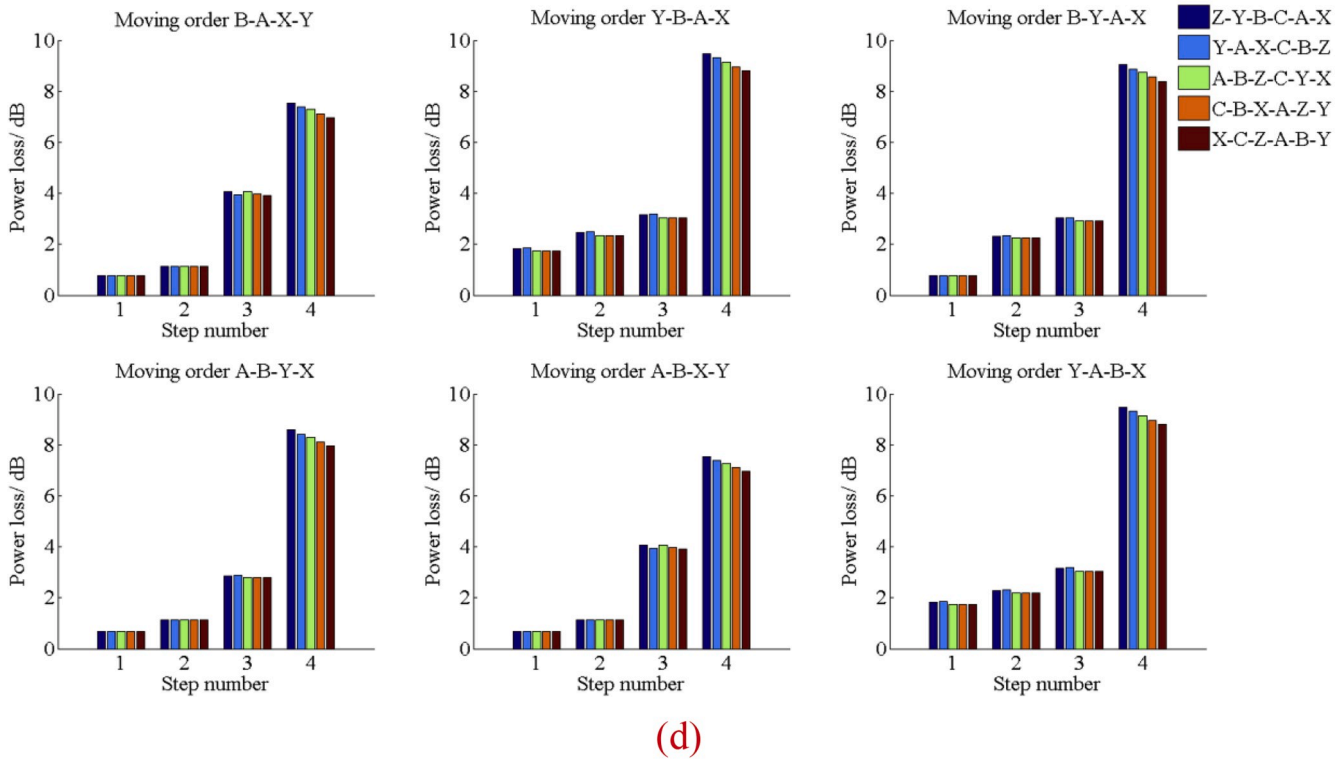

Fig. 6. (*continued*).

A direction and n_4 degrees in the B direction between two components, only 4 steps are required, such as X-Y-A-B or B-X-Y-A.

The optimal MO selection is conducted on the MPMS with configuration C-Z-O-X-Y-A-B using the procedures from the methodology section, with a translational step length of 0.1 mm and a rotational step length of 0.5°. To determine the optimal MO, the OPL value for four units in the first two steps are listed in Table 6.

Based on the results in Table 6, the average OPL for each direction at each step can be calculated, as shown in Table 7. It can be considered as a guide for coarse selection. The sensitivity index for each unit can also be deduced from this table, and by observing the increasing rate of the average OPL value for each unit in the first step, the sensitive order can

Table 5
OPL results at 4 steps.

Step number		Step 1	Step 2	Step 3	Step 4
Power loss value of different configurations/dB	A-B-Z-C-Y-X	1.74	6.26	7.35	8.44
	C–B-X-A-Z-Y	1.73	6.11	7.19	8.28
	X-C-Z-A-B-Y	1.73	5.97	7.05	8.13
	Y-A-X-C-B-Z	1.86	6.45	7.54	8.64
	Z-Y-B-C-A-X	1.83	6.57	7.66	8.77

Table 6
Power loss values of various MOs in the first two steps.

Step number		Step 1	Step 2
OPL value of different MO/dB	*xy*	2.31	5.32
	yx	1.79	6.31
	yA	1.79	2.25
	xA	2.31	2.80
	yB	1.79	2.42
	xB	2.31	2.97
	Ax	0.69	2.91
	Bx	0.78	3.10
	Ay	0.69	2.10
	By	0.78	2.29
	AB	0.69	1.14
	BA	0.78	1.14

Table 7
Average OPL caused by X, Y, A, B units in the first two steps.

Step number		Step 1	Step 2
Average OPL/dB	Unit X	2.31	3.02
	Unit Y	1.79	1.98
	Unit A	0.69	0.44
	Unit B	0.78	0.58

be arranged as X>Y>B>A. For the X unit, the average OPL value in the first step is larger than that in the second step, which means that the X unit should be set at the beginning of the moving sequence. Using the same procedures, the Y unit should also be set in the beginning of the moving sequence, and the A and B units should be arranged at the end of the MO. According to the methodology, the change in the speed of the DOFs is X>A>B>Y; therefore, X should be set at the beginning of the MO. The selection scale is shrunk from 24 MOs to 6 MOs, with X at the 1st place of the sequence.

The 1st place is determined, after which the last three places are considered. The average OPL values generated in the first two steps within the selection scale are listed in Table 8. Using the same procedure, the sensitive order for the remaining three units is Y>B>A, and the average OPL value of the Y unit in the first step is smaller than that in the second step; in addition to these two steps, Y is the faster decreasing direction. Therefore, the Y unit should be set at the end of the sequence. The selection scale is shrunk again to two MOs, with X at the beginning and Y at the end.

Table 8
Average OPL caused by Y, A and B units in the evaluated steps within the selection scale.

Step number		Step 1	Step 2
Average OPL/dB	Unit Y	3.01	2.97
	Unit A	0.49	0.77
	Unit B	0.66	0.98

Repeating these procedures, the optimal MO can be obtained, i.e. X-A-B-Y. This selection method is verified by comparing the analytical result with the results of 24 MOs listed in Table 9.

Therefore, a novel approach to analyse the most accurate MO is proposed. The procedures of this method are described below.

1. Assuming there are *n* motions in an MO, and these movements have a total of *n* motion steps. First, present the table of the average power loss of various motions for all cases in each step, and rank the sensitive indexes for units with various motions depending on the OPL value caused by these motions in step 1. Calculate the variation in the speed for each unit, then compare the results of *n* motions and find the fastest changing motion between step 1 and step 2. If the average OPL value of this motion is increasing, this motion should be ranked at the first place of the moving sequence. On the contrary, if the average OPL value of this motion is decreasing, this motion should be ranked at the last place of the moving sequence. It should be noted that if there are repeated motions in an MO, these motions should be considered as separate individual motions, each of which takes one place in the MO.
2. After the first or last place of the moving sequence is determined, the selection range is narrowed ($n = n$ - 1). List in a table the average OPL for the other *n*-1 motions for the selected cases in the remaining steps. Then, rank the sensitive order for these units again. Based on the same rule to place motion, the chosen motion can be arranged in the first or the last place in the left unchosen *n*-1 places in the moving sequence.
3. The selection range is narrowed again after procedure 2. Then, repeat procedure 2 to determine the remaining places of the moving sequence.

From the discussion of the quality of MOs, the conclusions can be as shown in Fig. 7.

There are two ways to weigh the MO. The first is the accuracy. If the final deviation is low, it means that the MO is good. The second is efficiency. Sometimes, for different MOs, the final orientations are close, or the engineer concentrates on the deviation propagation process. Based on this consideration, there is a deviation trend, and the moving process is also important. If achieving an adequate efficiency is the primary concern, the optimal MO selection should be changed. By the 5th procedure in the methodology section, the sensitive order in the first

Table 9
OPL values for various MOs in four steps.

Step number		Step 1	Step 2	Step 3	Step 4
OPL value of different MO/dB	*xyAB*	2.31	5.32	6.12	7.42
	yxAB	1.79	6.31	7.15	8.48
	yAxB	1.79	2.25	7.46	8.79
	yABx	1.79	2.25	3.11	9.18
	xAyB	2.31	2.80	5.71	6.99
	xABy	2.31	2.80	3.71	6.65
	yBxA	1.79	2.42	7.74	8.85
	yBAx	1.79	2.42	3.12	9.18
	xyBA	2.31	5.32	6.37	7.43
	xBAy	2.31	2.97	3.71	6.67
	xByA	2.31	2.97	6.01	7.06
	AxyB	0.69	2.91	5.98	7.27
	AxBy	0.69	2.91	3.82	6.92
	BxyA	0.78	3.10	6.33	7.39
	BxAy	0.78	3.10	3.86	7.00
	AyxB	0.69	2.10	7.00	8.32
	AyBx	0.69	2.10	2.95	8.71
	ByxA	0.78	2.29	7.34	8.43
	ByAx	0.78	2.29	2.99	8.76
	ABxy	0.69	1.14	3.99	7.28
	AByx	0.69	1.14	2.84	8.31
	BAxy	0.78	1.14	3.99	7.29
	BAyx	0.78	1.14	2.85	8.32
	yxBA	1.79	6.31	7.40	8.49

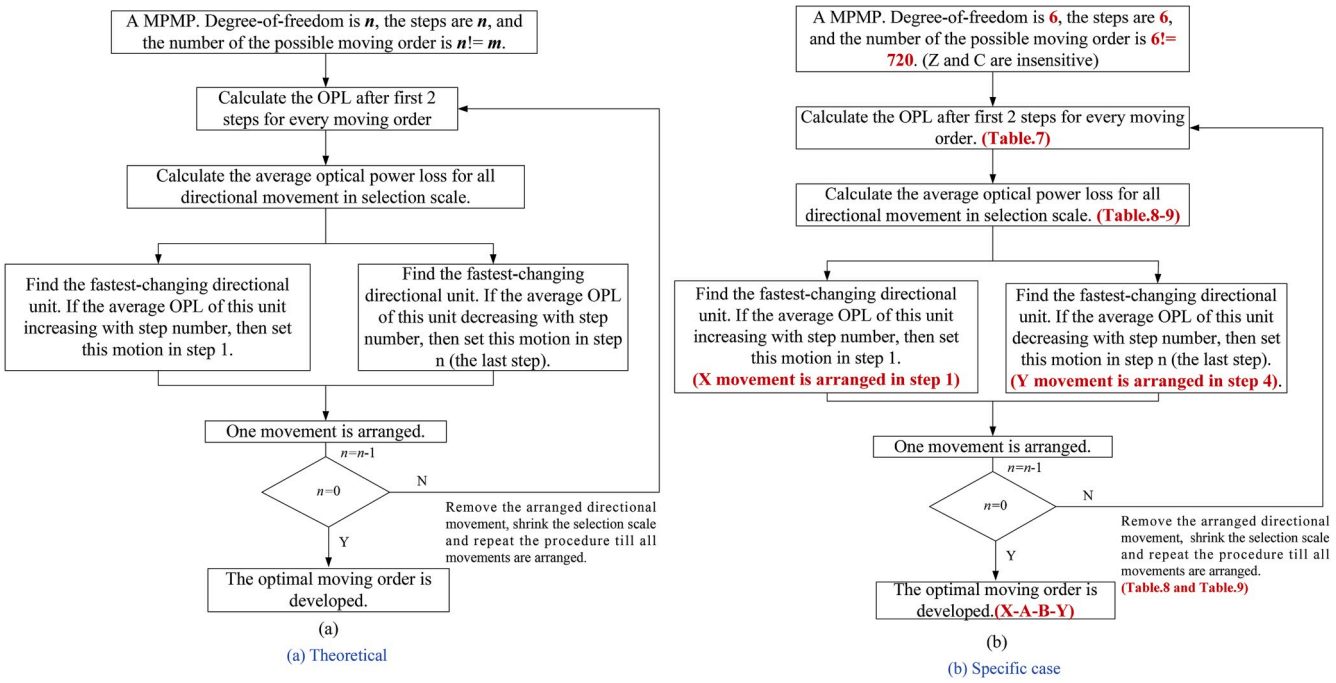

Fig. 7. MO selection procedure considering accuracy.

step is X>Y>B>A (see Table 6). The A and B units are similar units. Thus, the X unit and Y unit are arranged at the 4th and 3rd places, respectively, and the selection scale is shrunk to A-B-Y-X and B-A-Y-X. Table 10 lists the average OPL values of the A and B units in the remaining two steps.

By calculating the values from Table 10, the increasing speed of A equals that of B, while the sensitive index of A is smaller than B. Thus, B is arranged at the back of A. The optimal MO is A-B-Y-X, which is in accordance with the results in Table 10. The MO selection method with respect to efficiency is validated.

3.5. Experiment procedure

To prove the validation of the new approach and the corresponding conclusion above, a series of experiments are conducted, and the arrangement is as shown in Fig. 8. The To-Can packaging module is an alignment between two coupling units, and the OPL is measured using an optical power meter. The orientation of the coupling unit is controlled by an MPMS. All the data are shown on the display screen.

There are two ways to weigh the MO, accuracy and efficiency. Based on Eq. (9) and Eq. (10), if ω and μ are defined, the MO can be developed precisely. First, the MO should be analysed separately according to accuracy and efficiency.

According to the methodology, the sensitivity of four units should be concentrated within experimental results of 24 moving orders. Table 11 lists the power loss values of different MOs in the first two steps. In the OPS, according to the characteristics in the optical alignment, the values in Table 11 are processed as follows, and this step is to find the most accurate MO.

The average power loss values generated by four motion units in each step are listed in Table 12.

Table 10
Average OPL caused by A, B units in the evaluated steps within the selection scale.

Step number		Step 1	Step 2
Average OPL value/dB	Unit A	0.69	0.36
	Unit B	0.78	0.45

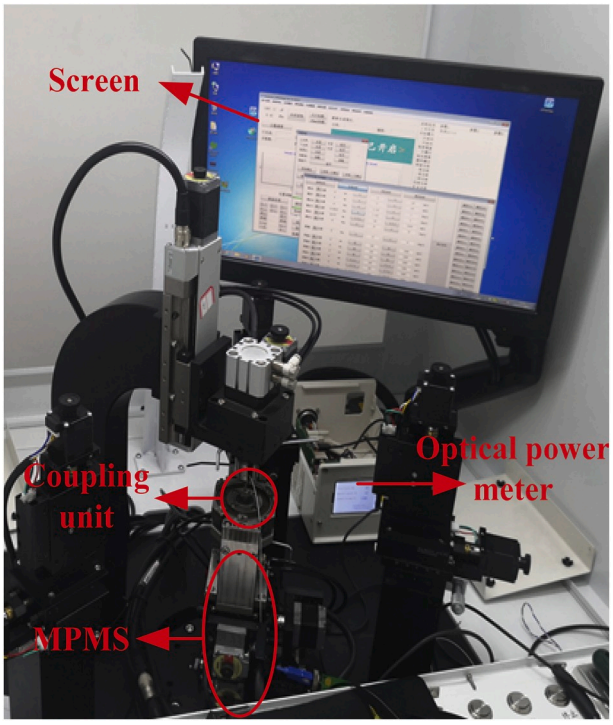

Fig. 8. Arrangement of the LWS system.

From Table 12, the sensitive order for four units is Y>X>B>A, and the changing speed order is X>Y>B>A; then, the X unit is first arranged. Because the average OPL of the X unit in the first step is larger than that in the second step, X is arranged in the last place in the motion sequence. Therefore, the selection scale is narrowed to six options, which are Y-A-B-X, Y–B-A-X, A-Y-B-X, A-B-Y-X, B–Y-A-X and B-A-Y-X.

After determining the X unit, the average OPL values generated by Y, B and A units in the first two steps within the evaluated scale are listed in Table 13.

Table 11
OPL values of various MOs in four steps.

Step number		Step 1	Step 2
OPL value of different MO/dB	*xy*	4.05	6.5
	yx	5.3	6.76
	yA	5.17	6.65
	xA	4.12	4.4
	yB	5.33	5.48
	xB	4.17	5.09
	Ax	1.12	4.44
	Bx	1.28	5.30
	Ay	0.98	6.84
	By	1.29	5.5
	AB	1.1	1.34
	BA	1.22	1.505

Table 12
Average OPL caused by X, Y, A, B units in first two steps.

Step number		Step 1	Step 2
Average OPL/dB	Unit X	4.12	2.93
	Unit Y	5.27	4.19
	Unit A	1.07	0.68
	Unit B	1.26	0.44

Table 13
Average OPL values of Y, A and B motions in the evaluated steps.

Step number		Step 2	Step 3
Average OPL/dB	Unit Y	5.22	4.95
	Unit A	1.04	0.94
	Unit B	1.28	0.24

Using the same procedure, B is arranged in the 3rd place in motion sequence. The selection scale is shrunk to Y-A-B-X and A-Y-B-X. In addition, the average OPL values generated by the Y and U units in the first two steps within the evaluated scale are listed in Table 14.

By repeating the procedures, the most accurate MO is Y-A-B-X. The experimental results are given in Table 15, which verifies this analytical result.

By considering the efficiency and accuracy, four typical MOs are proposed based on the data in Table 15 for comparison, as shown in Fig. 9.

Using the optical power meter, the OPL after each step can be measured. In Fig. 9(a), (b), (c), and (d), four typical MOs are denoted by the poorest efficiency, the highest efficiency, the highest accuracy and the poorest accuracy, respectively. Fig. 9(a) and (b) have the largest and smallest areas, respectively. Fig. 9(c) and (d) respectively have the lowest (8.82 dB) and highest values (17.65 dB) after step 4. Thus, by considering different requirements, the optical MO can be developed. The results can also be obtained using Eq. (9) and Eq. (10).

From Table 12 the sensitive order in the first step is Y>X>B>A, and it should be noted that the most efficient MO is A-B-X-Y. These analytical results based on the MO analytical laws are in accordance with the experiment results. Based on the methodology, if $\omega = 1$ and $\mu = 0$, the optimal MO is Y-A-B-X, and if $\omega = 0$ and $\mu = 1$, the optimal MO is A-B-X-Y. Meanwhile, if $0 < \omega < 1$ and $0 < \mu < 1$, the optimal MO is selected from among the range Y-A-B-X to A-B-X-Y.

Hence, this methodology was verified by performing practical experiments. This method can not only be used in a real alignment procedure to plan the MO, but it can also be introduced in simulations associated with alignment algorithms to predict the alignment trajectory. The results in Fig. 10 indicate that the computational volume for selecting the optimal MO can be reduced significantly using the new approach. For the multi-axis motion system, if the number of DOFs is low, the calculation volume of two approaches is relatively low. However, for 5- or 6-axis system, the novel approach can result in a large volume savings to select the optimal MO. For numbers 5 and 6 on the left part, calculation volumes of 583 and 4286 are respectively needed, and for the right part, calculation volumes of only 85 and 193 are needed. The results are the same and are precise. Therefore, the novel approach can not only result in savings with respect to the computational volume, but it also guarantees systematic accuracy.

For different configurations, an optimal sequence strategy can be made to meet the accuracy and efficiency requirements. Although the introduction of the strategy is a little complicated, it can search the optimal moving sequence step by step.

However, it does have limitation. First is the computational volume in step searching. The computational volume will increase depending on the DOF increasing, which means for a complicated motion system, more computational volume will be cost. Second is the computational volume in step length. The smaller the step length is, the more accurate the motion sequence is, but the more computational volume cost. More researches will be developed to enlarge the application of the novel approach in future.

Table 14
Average OPL caused by A and B units in the evaluated steps within the selection scale.

Step number		Step 1	Step 2
Average OPL value/dB	Unit Y	5.11	5.79
	Unit A	1.01	1.55

Table 15
Experimental results of various MOs in four steps.

Step number		Step 1	Step 2	Step 3	Step 4
OPL of different MO/dB	*xyAB*	3.95	6.53	7.29	7.45
	yxAB	5.25	6.73	7.38	7.6
	yAxB	5.24	6.64	7.2	7.52
	yABx	5.11	6.66	6.8	7.33
	xAyB	4.09	4.44	7.19	7.45
	xABy	4.16	4.36	4.42	7.51
	yBxA	5.33	5.43	6.91	7.42
	yBAx	5.33	5.53	6.81	7.55
	xyBA	4.16	6.6	6.9	7.46
	xBAy	4.17	5.11	5.17	7.51
	xByA	4.17	5.07	6.93	7.45
	AxyB	1.13	4.33	7.32	7.55
	AxBy	1.11	4.55	5.2	7.56
	BxyA	1.32	5.35	6.98	7.63
	BxAy	1.25	5.26	5.29	7.61
	AyxB	0.96	6.88	7.37	7.54
	AyBx	1.01	6.8	6.87	7.67
	ByxA	1.26	5.56	7	7.54
	ByAx	1.32	5.44	6.95	7.66
	ABxy	1.12	1.32	5.3	7.42
	AByx	1.08	1.37	7.05	7.66
	BAxy	1.2	1.43	5.36	7.62
	BAyx	1.24	1.58	6.98	7.59
	yxBA	5.35	6.8	7.11	7.46

4. Conclusion

In this paper, a systematic error modeling method was introduced to mathematically describe the poses and positions of a multi-degree-of-freedom platform. The units' configuration was developed in MPMS based on this method, and some laws of MO which are deduced from the analysis of MO are proposed. These laws were verified by performing both simulation and practical experiments. Based on these experimental and analytical results, the conclusions are summarized as follows:

1. The units' configuration has been analysed, and using the orthogonality test and performing simulations, it is proven that it does not influence the MO analysis. This is beneficial to the future research on trajectory planning for optical module alignment.

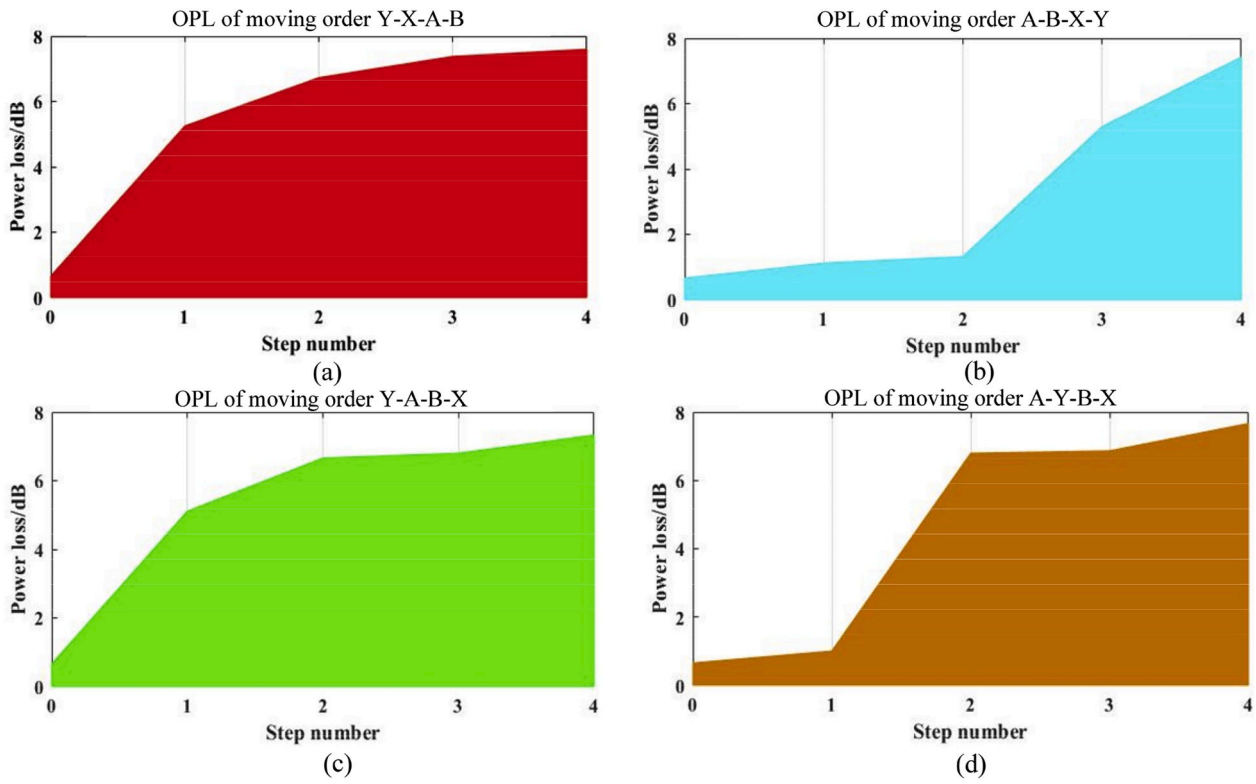

Fig. 9. Comparison of error propagation values of four MOs.

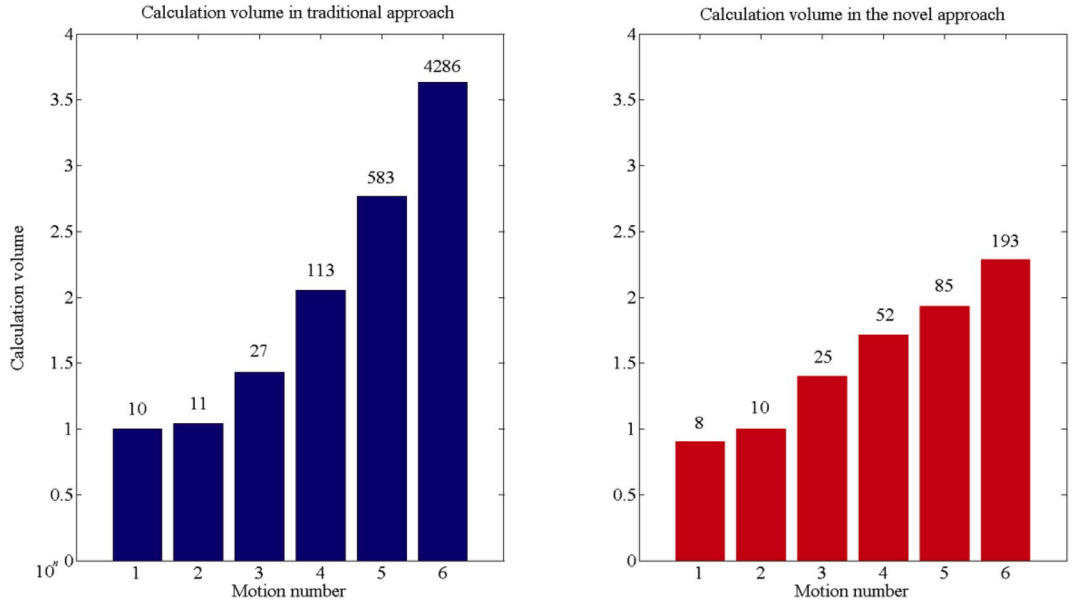

Fig. 10. Comparison of traditional and new approaches in terms of calculation volume.

2. The relationship between the efficiency and the accuracy of the alignment was developed, and this is useful for realizing efficiency improvements of motion platforms. By utilizing the approach, the efficiency and accuracy can be balanced with different requirement, which is significant for controlling the MPMS in motion procedure (Fig. 1 and Eq. (4) to Eq. (10)).
3. A method for planning the most accurate MO for alignment is proposed. According to the theoretical analysis above, this analytical method was carried out by using simulations and practical experiments. Based on this proposed method, optimized alignment path prediction can also be achieved associated with alignment algorithms.
4. An equation for achieving trajectory planning was proposed according to the specific requirements of optoelectronic packaging systems. This equation enables the planning of MOs aimed at different targets.

This approach provides a new thought for finding the MO through calculating the deviations step-by-step, and considers the effect between efficiency and accuracy with different requirements. In future work, an

algorithm based on the MO analytical laws and other alignment algorithms will be developed to enhance the performance of MPMS. In addition, the definition of the optical power coupling field should be developed and researched. It is important to fully understand the coupling patterns and the laws in alignment path searching; in this way, the high-precision packaging for optical devices and high-quality operation for MPMS can be realized.

Declaration of competing interest

The authors declared that they have no conflicts of interest to this work.

We declare that we do not have any commercial or associative interest that represents a conflict of interest in connection with the work submitted.

Acknowledgement

This research is supported by the National Natural Science Foundation of China (Grant No. 51705149) and the Natural Science Foundation of Hunan province (Grant No. 2018JJ3168).

References

[1] Zhao D, Bi YB, Ke YL, et al. An efficient error compensation method for coordinated CNC five-axis machine tools. Int J Mach tools & Manuf. 2017;123:105–15.
[2] Hale LC. Principles and techniques for designing precision machines. California, U. S: Ph.D thesis, University of California; 1999.
[3] Tang H, Li CP, Zhang ZL, et al. A novel geometric error modeling optimization approach based on error sensitivity analysis for multi-axis precise motion system. J Mech Sci Technol 2019;33(7):3435–44.
[4] Vogl GW, Jameson NJ, Archenti A, et al. Root-cause analysis of wear-induced error motion changes of machine tool linear axes. Int J Mach tools & Manuf. 2019;143:38–48.
[5] Yang B, Zhang GB. Kinematic modeling and machining precision analysis of multi-axis CNC machine tools based on screw theory. Mech Mach Theor 2019;140:538–52.
[6] Zhong XM, Liu HQ. Influence and error transfer in assembly process of geometric errors of a translational axis on volumetric error in machine tools. Measurement 2019;140:450–61.
[7] Huang J, Lu YA, Zhu LM. Real-time feedrate scheduling for five-axis machining by simultaneously planning linear and angular trajectories. Int J Mach tools & Manuf. 2018;135:78–96.
[8] Tseng CY, Wang JP. Automation of multi-degree-of-freedom fiber-optic alignment using a modified simplex method. Int J Mach Tool Manufact 2005;45(10):1109–19.
[9] Chun J. Fiber optic active alignment method based on a pattern search algorithm. Opt Eng 2006;45(4):045005.
[10] Lin CS, Tsai JM. The design and application of an automatic optical inspection system for the advanced fiber coupler assembly manufacturing process. Int J Precis Eng Manuf 2014;15(9):1847–54.
[11] Wang WX, Hu CX, Zhou K, et al. (B.6)Corner trajectory smoothing with asymmetrical transition profile for CNC machine tools. Int J Mach Tools Manuf 2019;144:103423. Article.
[12] Pham VD, Song CK. A novel dynamic model for multiple configurations of machine tools using a coordinate transformation method. Int J Adv Manuf Technol 2018;95:27–42.
[13] Z Wang T, Wu CY, et al. Configuration design and accuracy analysis of special grinding machine for thin-walled small concave surfaces. Precis Eng 2019;56:293–302.
[14] Tang H, Zhang ZL, Li CP, et al. A geometric error modeling method and trajectory optimization applied in laser welding system. Int J Precis Eng Manuf 2019;20(8):1423–33. https://doi.org/10.1007/s12541-019-00151-8.
[15] Mukhopadhyay S, Sarkar SN. Coupling of a laser diode to monomode elliptic core fiber via upside down tapered microlens on the fiber tip: estimation of coupling efficiency with consideration for possible misalignments by ABCD matrix formalism. Optik 2019;121(2):142–50.
[16] Yang H, Chen C, Ro R. Investigation of the efficient coupling between a highly elliptical Gaussian profile output from a laser diode and a single mode fiber using a hyperbolic-shaped micro lens. Optic Laser Technol 2010;42(6):918–26.
[17] Wu YF, Zhao H, Zhang C, et al. Optimization analysis of structure parameters of steam ejector based on CFD and orthogonal test. Energy 2018;151:79–93.